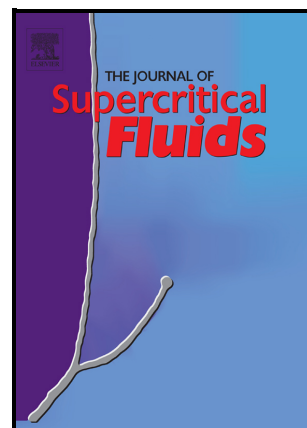# Journal Pre-proof

Understanding sulfonated kraft lignin re-polymerization by ultrafast reactions in supercritical water

Tijana Adamovic, Xuhai Zhu, Eduardo Perez, Mikhail Balakshin, Maria José Cocero

Please cite this article as: Tijana Adamovic, Xuhai Zhu, Eduardo Perez, Mikhail Balakshin and Maria José Cocero, Understanding sulfonated kraft lignin re-polymerization by ultrafast reactions in supercritical water, *The Journal of Supercritical Fluids*, (2022) doi:https://doi.org/10.1016/j.supflu.2022.105768

This is a PDF file of an article that has undergone enhancements after acceptance, such as the addition of a cover page and metadata, and formatting for readability, but it is not yet the definitive version of record. This version will undergo additional copyediting, typesetting and review before it is published in its final form, but we are providing this version to give early visibility of the article. Please note that, during the production process, errors may be discovered which could affect the content, and all legal disclaimers that apply to the journal pertain.

Understanding sulfonated kraft lignin re-polymerization by ultrafast reactions in supercritical water.

Tijana Adamovic[a] Xuhai Zhu[b,c] Eduardo Perez[a,d] Mikhail Balakshin[b] and Maria José Cocero[a,]*

[a]BioEcoUva Bioeconomy Research Institute, Press Tech Group, University of Valladolid, Doctor Mergelina s/n, 47011 Valladolid, Spain

[b] Department of Bioproducts and Biosystems, School of Chemical Engineering, Aalto University, P.O. Box 16300, 00076 Aalto, Finland

[c] State Key Laboratory of Catalysis, Dalian National Laboratory for Clean Energy, Dalian Institute of Chemical Physics, Chinese Academy of Sciences, Dalian, Liaoning 110623, P. R. China

[d] Department of Physical Chemistry, Faculty of Sciences, Complutense University, Avda Complutense s/n, 28040 Madrid, Spain

Corresponding author: Maria José Cocero

e-mail: mjcocero@iq.uva.es

Abstract

Re-polymerization reactions are a commonly reported issue on the way to the higher recovery of monomers from lignin. The reactivity of monomers obtained from lignin depolymerization and their contribution to the re-polymerization in supercritical water (SCW) was investigated. Sulfonated Kraft lignin (SKL) was used along with four monomers: vanillin, vanillic acid, vanillyl alcohol and acetovanillone. Indulin Kraft lignin was also employed as the reference to

understand the re-polymerization of SKL in SCW. The formation of diarylmethane structures was detected in HSQC spectra of solid residue after the SCW process. Lignin released fragments with free phenolic β-O-4 structures, as well as the monomeric product vanillyl alcohol are involved with the formation of o-o´ and o-p´ diarylmethane structures. Chemical structure of Kraft lignin and its polymeric product after the SCW process was remarkably similar, as shown by HSQC, indicating that re-polymerization reactions occur through cross-linking polymerization, mainly in their fractions of low molecular weight products.

Keywords:

diarylmethanes structures • sigma lignin • vanillin • vanillic acid • vanillyl alcohol • acetovanillone

1. Introduction

An uncertain future based on fossil fuels and growing environmental awareness are directing our forces towards the development of more sustainable energy and chemical sources. Biomass is the renewable source of carbon [1] and thus the potential renewable source for chemicals and fuels. The development of biorefinery as ``the sustainable processing of biomass into a spectrum of marketable products and energy``[2] is a prudent way toward a sustainable future. Lignocellulosic biomass is the most abundant biomass source composed of three main components: cellulose, hemicellulose and lignin. To build a biorefinery competitive with a petroleum refinery, an effective conversion and utilization of all biomass fractions is crucial.

Lignin is the most abundant aromatic polymer in nature. Its aromatic moieties attract remarkable attention as lignin could play an important role as a sustainable source for aromatic chemicals. The scientific community has recognized this potential, shown by the big

number of articles discussing different technologies and strategies of lignin valorization. Among all possible lignin applications, its efficient conversion to low-molecular-weight aromatics is very popular. However, it is also the most challenging and complex objective due to the lignin technology barriers [3] as well as economic issues [4]. Those barriers arise from the very complex and recalcitrant lignin nature, influenced by many factors, among which are the methods used to isolate lignin from biomass.

Kraft process is the dominant pulping procedure used to separate cellulose fibers from lignin, with an estimated global production of 130 Mt/y (as extracted in black liquor; about 5-15% of it can be isolated from black liquor while the rest is needed to be incinerated for the Kraft chemicals recovery) [5]. Advantages of the Kraft process over others in the Pulp and Paper Industry are: high quality of the pulp, insensitivity to the wood species and possibility of recovery of chemicals and energy [6]. In the Kraft process, lignin and part of hemicelluloses of the wood chips are dissolved in the solution of sodium hydroxide and sodium sulphide resulting in the isolation of cellulose fibers. During the treatment, the hydroxide and hydrosulfide anions react with the lignin causing the polymer to break into smaller fragments [7]. Isolated lignin from the Kraft process undergoes many degradation and condensation reactions [8–11]. One of the obstacles to the further processing of Kraft lignin is its limited solubility in water. As solubility is an important factor that facilitates lignin handling, sulfonation of Kraft lignins has become practice [12].

Numerous strategies have been utilized to break down the lignin molecule to obtain valuable aromatic compounds. Methods used for lignin depolymerization can be listed as thermochemical methods (pyrolysis, hydrogenolysis, hydrolysis, etc.), microwave-assisted depolymerization, methods using chemicals or catalysts (acid-catalyzed, base-catalyzed, metallic-catalyzed, ionic liquid-assisted catalyzed, methods using hydrogen peroxide as catalyst) and biological methods (bacteria, fungi, enzymes) [13]. Despite the availability of lignin and all the effort involved in obtaining aromatic compounds from it, the scaling up of

the processes involved in lignin deconstruction is very challenging, due to the difficulties in depolymerization and product separation [14]. Process limitations and complex lignin structure are the main difficulties to the successful valorization of lignin into high-value aromatic chemicals. Examples of process limitations for some technologies are: harsh conditions in the sense of long reaction time, high pressure and temperature and environmental concerns for acid and base-catalyzed depolymerisation; use of expensive (noble metal-based catalyst), the lack of mass transfer from lignin feedstocks to the catalytic surface and the recyclability of the heterogeneous catalyst for heterogeneously catalyzed depolymerisation; low yield of products, possible recombination/re-polymerization of lignins and lignin fragments and the feasibility of product separation in the case of oxidative depolymerisation; cost, environmental issues and recyclability for processes that use ionic liquids [14,15].

Water at elevated temperatures and in a supercritical state has been recognized as a potential reaction medium for lignin depolymerization [16–22]. This green technology that uses water as solvent overcomes many limitations of applied conventional processes, firstly regarded the use of toxic and expensive catalysts and solvents. The properties of SCW differ from those of ambient liquid water. SCW behaves as many organic solvents due to the low value of dielectric constant [23]. Properties of subcritical and supercritical water vary over a wide temperature and pressure range, which gives the possibility to adjust medium identity simply by setting those parameters [24]. Another important benefit of SCW is its ability to dissolve both organic compounds and gases, thus the reaction occurs in a single phase overcoming the limitation of mass transfer. Moreover, high temperatures can greatly enhance the reaction kinetics so a small continuous reactor can be used for very short reaction times.

Different works discussing depolymerization of lignin in SCW reported an increased yield of solid residue and decreased yield of monomers over reaction time due to the re-polymerization reaction. They also reported that liberated formaldehyde could promote re-polymerization and proposed the use of capping agents such as phenol and p-cresol to prevent

undesired re-polymerization and increase the yield of oil enriched in monomers [25–28]. Keeping a short reaction time is essential in lignin depolymerization to avoid undesired re-polymerization reactions and to favor monomer recovery. Previous results demonstrated that Sulfonated Kraft lignin (SKL) can be successfully converted into aromatic monomers via ultrafast depolymerization in SCW, keeping the reaction time under 500 ms [29]. The results showed that the total aromatic yield based on lignin was 10.5 % w/w. It was found that the optimum reaction time for lignin depolymerization was 300 ms. At longer reaction times however, the yield of the monomeric fraction decreases, followed by an increase in the yield of the heavier fraction, as a result of possible product recombination and re-polymerization. The yield of monomeric units starts to decrease after the optimum point, suggesting that these units play an active role in re-polymerization [29].

Re-polymerization reactions present an important limiting factor on the way to higher recovery of aromatics from lignin, which faces every depolymerization method. The mechanism of re-polymerization reactions in SCW is still unclear and its understanding is one way to prudently govern the depolymerization reaction towards the high yield of monomers. In this paper, we focus our interest on a better understanding of re-polymerization processes in SCW. In particular on the reactivity of a mixture of model compounds in presence of lignin to find out if they react between themselves or if they react with other lignin fragments. On the other hand, it was desired to understand the main changes that occur in the SKL structure during the SCW process. This was analyzed using FTIR, Gel Permeation Chromatography (GPC) and 2D HSQC NMR.

2. Experimental section

2.1 Materials

Technical lignins and model compounds used in the experiments are listed in Table 1. Sodium hydroxide used as a catalyst, and ethyl acetate (>99%) used for sample fractionation were purchased from PanReac. Distillate water type III was used as a reaction medium. Acetic acid, sodium acetate, acetonitrile and methanol used in HPLC and GPC analysis were all purchased from Sigma Aldrich. Specifications can be found in Table 1.

**Table 1.** Technical lignins and model compounds used in the study

Compound	CAS	Purchased from	Purity
Vanillin	121-33-5	Sigma Aldrich	99.9
Vanillic acid	121-34-6	Sigma Aldrich	99.8
Vanillyl alcohol	498-00-0	Sigma Aldrich	99.9
Acetovanillon	498-02-0	Sigma Aldrich	99.8
Sulfonated Kraft Lignin	8068-05-1	Sigma Aldrich	Lot MKCG9481
Kraft Lignin (Indulin AT)		Ingevity (formerly MeadWestvaco)	

2.2 Methods

2.2.1 Experimental setup

Experiments were carried out in a continuous lab-scale plant with a sudden expansion micro-reactor (SEMR) shown in Figure 1. The design of the plant allows sudden start and termination of the reaction by sharp temperature changes. The sudden start is achieved by the mixing of SCW and the compressed lignin/model compound solution in the T-junction just at the entrance of the reactor. The flow of water and lignin solution is controlled by high-pressure piston pumps whose operating ranges are previously calibrated using water. The termination is achieved by sudden decompression using a high-temperature needle valve,

resulting in a Joule-Thomson effect, so that after the reactor the temperature decrease to approx. 200 °C. In this way, it is possible to achieve a short reaction time and avoid heating and cooling slopes that prevent its accurate control. After the decompression valve, a heat exchanger was installed to cool the sample further down to room temperature. Each sample was taken after the reactor has reached a steady state, which was controlled following values of temperature in pressure over time. Each sample has been taken in duplicate. The mass balance is presented in supplementary. The maximum operating conditions of the plant are 425 °C and 300 bar, with a maximum capacity of 3.6 kg/h of lignin solution. More details about the setup can be found in a previous report [30].
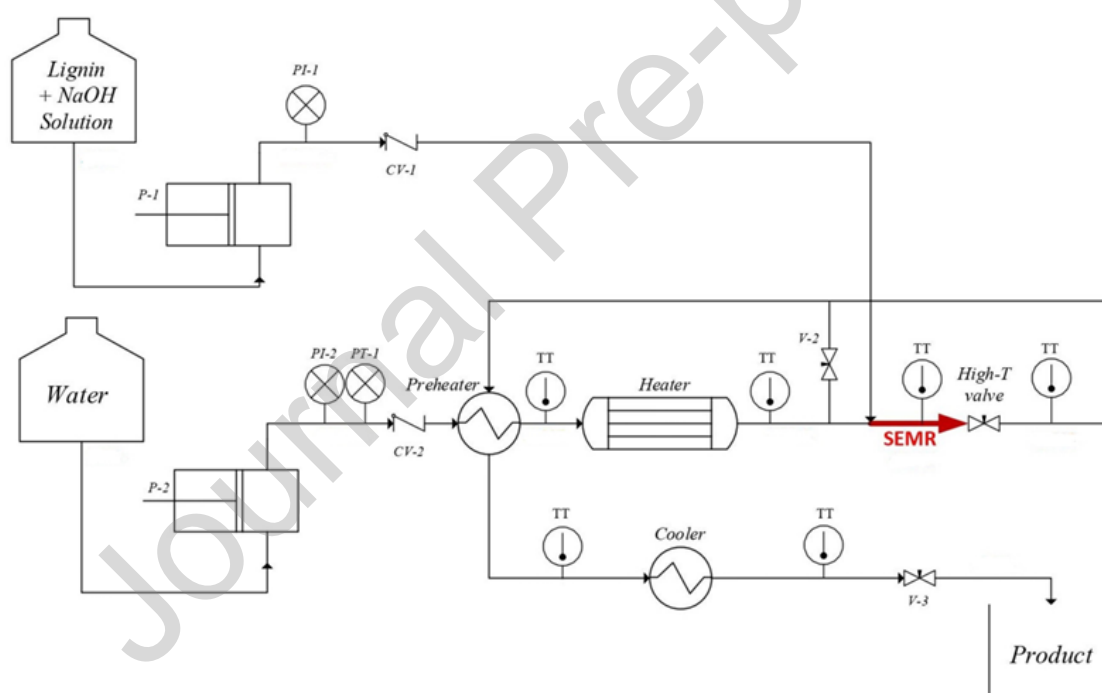

Figure 1. Flow diagram of lab-scale continuous plant with SEMR

2.2.2 Experimental procedure

The chosen model compounds for these experiments were four guaiacyl type monomers: vanillin, vanillin acid, vanillyl alcohol and acetovanillone. Vanillin and acetovanillone are the main model compounds isolated in the previous studies of our research group. Vanillyl alcohol is a model compound of lignin moieties and a reactive intermediate that has been

proposed to play an important role in lignin condensation [31]. Aromatic acids such as vanillic acid have been usually found in hydrothermal reactions. The water solutions of reagents were prepared in 0.1M sodium hydroxide. Two reference experiments were performed, one just with 5% w/w SKL, and another with an equimolar mixture of the four model compounds (MC) with a total concentration of 2 % w/w. The total concentration (MC + SKL) for the rest of the experiments was 5 % w/w, with two different lignin to model compounds (SKL:MC) ratios of 1:4 and 2:3. The temperature in every experiment was 385 ±1 °C, the pressure was 254±2 bar and the residence time 360±20 ms. After the reaction, the sample is obtained in the liquid phase and further fractionated following a procedure similar to one reported by Perez and Tuck [32]. The sample was acidified to pH=2 using sulphuric acid, followed by centrifugation to separate the precipitated solid (s) and the aqueous (aq) fractions. The solid was then washed three times with acidified water (pH=2), which was collected and added to the liquid fraction. The solid was further extracted three times with ethyl acetate. The solvent after extraction was removed by a rotary evaporator and the solid obtained as the extract is called heavy oil fraction (s-E). The residue obtained after the extraction is called solid residue (s-R). The aqueous fraction was also extracted three times with ethyl acetate. The solvent of the organic phase of this fraction was removed in a rotary evaporator and the obtained extract is named light oil (aq-E). The water phase fraction is called aqueous residue (aq-R), and it was discarded as usually does not provide significant information [32]. The procedure of sample fractionation explained here is simplified and presented in Figure 2.
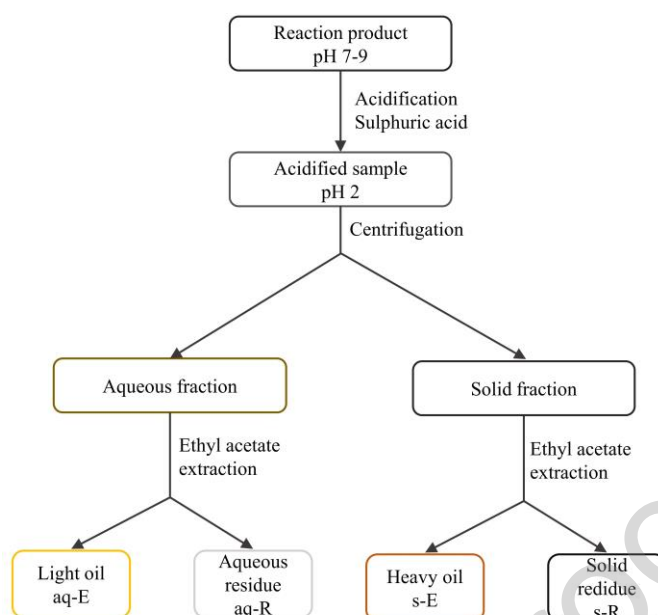
Figure 2. The procedure of sample fractionation after the reaction

2.2.3 Analysis

2.2.3.1 High-performance liquid chromatography (HPLC)

The concentration of the monomeric compounds after the SCW process was determined by HPLC. The analysis was performed using a method based on work from Perez and Tuck [32]. An Agilent TM 1100 series with an XterraTM C-18 column and a single wavelength UV detector at 230 nm were used. The mobile phase was the mixture of acetic acid / sodium acetate buffer and acetonitrile. The flow rate was 0.7 mL/min. Isocratic method (10 % acetonitrile) for the first 10 min; 10 – 20 min gradient method (10 to 50 % acetonitrile); 20-21 min, quickly decrease to initial conditions (50 to 10 %); 21-30 isocratic method (10% acetonitrile). The sample injection volume was 10 µL. Model compounds were identified and quantified using standards of vanillin, vanillic acid, acetovanillon, vanillyl alcohol and guaiacol, all purchased from Sigma Aldrich. The calibration curves of standards are given in Supplementary information. Every sample was analysed at least in duplicate.

2.2.3.2 Gel Permeation Chromatography (GPC)

The molecular weight distribution of the samples was determined by gel permeation chromatography (GPC). Jordi Gel Sulphonated Plus 10000 A 250 x 10 mm column was used

together with Waters IR detector 2414 (210 mm) and Waters dual λ absorbance detector 2487 (254 nm). The mobile phase was a solution of water and methanol in the ratio of 90:10 v/v, adjusted to pH = 12 at a flow rate of 1 mL/min (Perez and Tuck, 2018). Samples were dissolved directly in the eluent with a concentration between 2 and 6 mg/ml. The injection volume was 25 µl. The standards were not used in this analysis as the analysis amid to provide rather qualitative data and comparison of molecular weight among different samples [33].

2.2.3.3 Fourier Transform Infrared Spectroscopy (FTIR)

The equipment used for FT-IR analysis of lignin and s-R was a Bruker Tensor 27 with a diamond crystal. The analysis was performed at room temperature. The spectra are recorded in mode Attenuated Total Reflection (ATR). The baseline was corrected, and the peaks were normalized to the maximum peak.

2.2.3.4 2D HSQC NMR analysis

Two-dimensional 1H-13C correlation HSQC NMR experiments were performed with Bruker AVNEO 600 MHz spectrometers equipped with a cryogenically cooled 5 mm TCI probe head to identify and quantify the structure of lignin and their reaction product samples. Except for the 80 mg of SKL was fully dissolved in 0.6 ml of Dimethyl sulfoxide -d6/D2O mixture (5:1, vol.), 80 mg of other samples were fully dissolved only in 0.6 ml of Dimethyl sulfoxide -d6. A sensitivity-enhanced pulse program (hsqcetgpsisp.2) that utilizes shaped pulses for all 180° pulses on the proton channel was used in the acquisition. 1024 data points were acquired from 11 to 0 ppm in F2 (1H), with an acquisition time of 77.8 ms, and from 215 to 0 ppm in F1 (13C) with 256 increments, 36 scans, and a 2.0 s interscan delay, with a total acquisition time of 5 h 50 min in 298 K. The average value for one-bond J-coupling between protons and carbons were set as 145 Hz. All data were processed using Bruker BioSpin's Topspin 3.5 software. The spectra were calibrated using the central peak of the Dimethyl sulfoxide-d6 (δH 2.49 ppm, δc 39.5 ppm). Processing the final matrix to 2 k by 1 k

data points was performed by QSINE window functions in both F2 and F1. The known correlation peaks appearing in the HSQC spectra were assigned by referring to the NMR data of lignin model compounds in the NMR database of lignin model compounds and previous studies. The integrals were normalized to the integral of C2-H2 correlation at the 2-position of guaiacyl ring (G2), which are representative of all G-units as internal standard. Therefore, the results were relatively expressed per aromatic ring keeping in mind the semiquantitative character of the HSQC method. According to the integral value of G2 signal, the number of structural units could be relatively estimated by the following eqn. (1):

$$Ix\% = \frac{Ix}{I_{G2}} \text{ x } 100 \text{ \%}$$

(1)

Where Ix is the integral value of corresponding structural units. The integration was made in the same contour level condition (number of positive contour levels = 50, highest contour level = 100%, lowest contour level = 20).

3. Results and Discussion

3.1 Model compounds conversion

The reactivity of model compounds is followed by the conversion. The conversion of each compound is calculated by eqn. (2).

$$x = \frac{(c_{in} - c_{out})}{c_{in}}$$

(2)

Where is:

c_{in} –concentration of model compound inside the reactor (after mixing with SCW)

c_{out}– outlet concentration of model compound

In the first experimental set, the solution of MC mixture was processed in SCW. Herein the highest conversion is obtained in the order vanillyl alcohol > vanillin > vanillic acid > acetovanillone. Conversions of model compounds for this experimental run and in the run with SKL are presented in Figure 3. Guaiacol is detected in the HPLC chromatogram after the reaction as a product. This is expected as guaiacol was detected as a reaction product derived from the decomposition of some MC in SCW, for example, the decomposition of vanillic acid by decarboxylation reaction [34]. It has been proposed that other units used in this study e.g. vanillin and vanillyl alcohol could yield guaiacol by radical scissions [35,36].
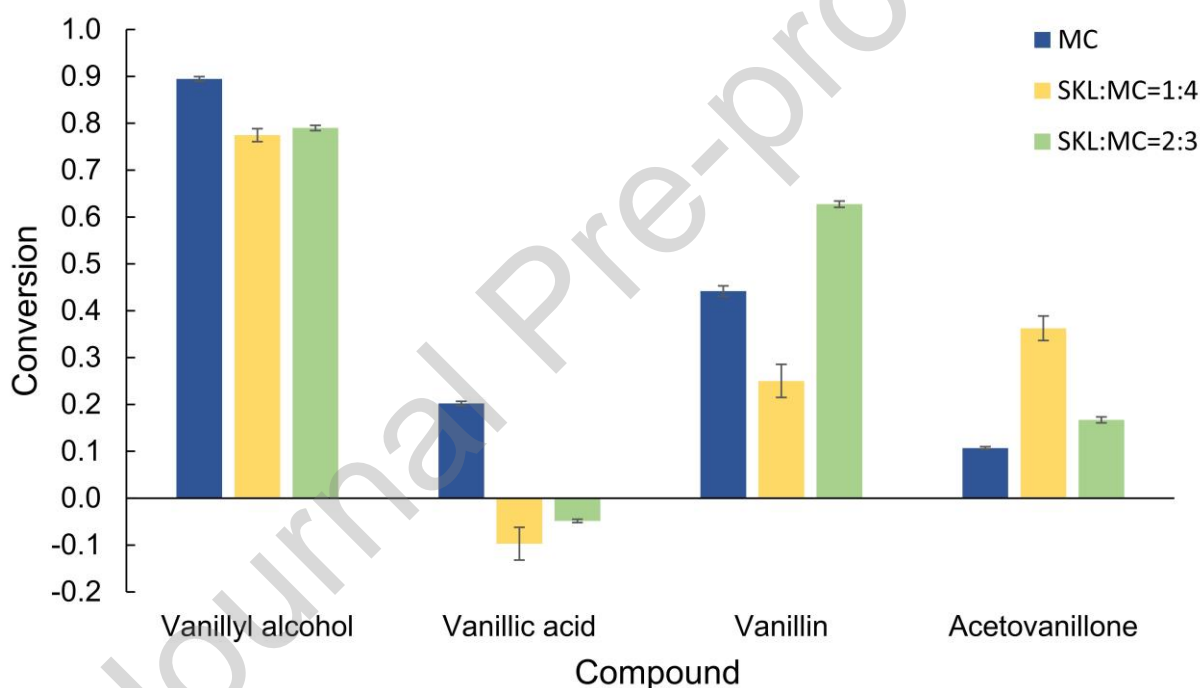
Figure 3. The conversion of model compounds in different experimental runs (error bars presented as standard error)

Adding SKL in the system change the conversion, while also conversion was different for different SKL:MC ratios. This may be the result of either MC reaction with SKL fragments or the latter inhibiting the monomer degradation. However, the indicial concentration of MC was different in the experiment with and without SKL, so a direct comparison of the conversion is not possible. During the lignin depolymerization reactions in SCW, it was observed that the

yield of obtained monomers decreases over reaction time as a result of re-polymerization reactions [29]. Conversion of vanillyl alcohol remains the highest one and similar for different SKL:MC ratios. The conversion of vanillic acid decreases significantly when SKL was introduced into the reactor, indicating vanillic acid production due to the presence of SKL. The net production of vanillic acid may be positive which could be explained by a certain amount of homovanillic acid production from SKL [35], which interferes with the HPLC signal of vanillic acid. In any case, these results suggest that SKL has a protective effect over vanillic acid. No clear trends could be obtained in the case of vanillin and acetovanillone conversion. Conversion of vanillin firstly decreases in SKL presence (SKL:MC = 1:4) and then increases from 0.25 to 0.63 when the concentration of SKL is higher (SKL:MC = 2:3). The opposite is observed for acetovanillone where the conversion firstly increases in presence of SKL and then decrease when more SKL is presented in the reactor.

3.2 Sample fractionation

After the reaction, the sample was fractionated into four fractions: aqueous residue (aq-R), aqueous extract (aq-E) called light oil, solid residue (s-R) and solid extract (s-E) called heavy oil. Every sample was fractionated in duplicate. s-R and s-E fractions together are marked as total solid and present heavier fractions of the sample. After the extraction, each fraction was dried at 105 °C and these values were used for further calculation. It is expected that the s-R is the fraction that contains the products from the re-polymerization reactions [29] for reaction times higher than the optimum. From Figure 4a, it can be seen that the s-R yield reaches the highest value for the experimental run with SKL. The yield decreases when MC are introduced into the reaction mixture, i.e., decreases by lowering the SKL concentration compared to the concentration of MC. The yield of the s-E fraction is around 35% and thus similar for every experiment (Figure 4c). This yield is based on the total mass inside the reactor (MC + SKL). If we however present this yield based on the mass of SKL inside the reactor (Figure 4d), it can be seen that for the ratio SKL:MC = 1:4 the yield of s-E fractions

exceeds 100%, indicating that MC upgrade to the heavier fraction. This contributes mainly to s-E.
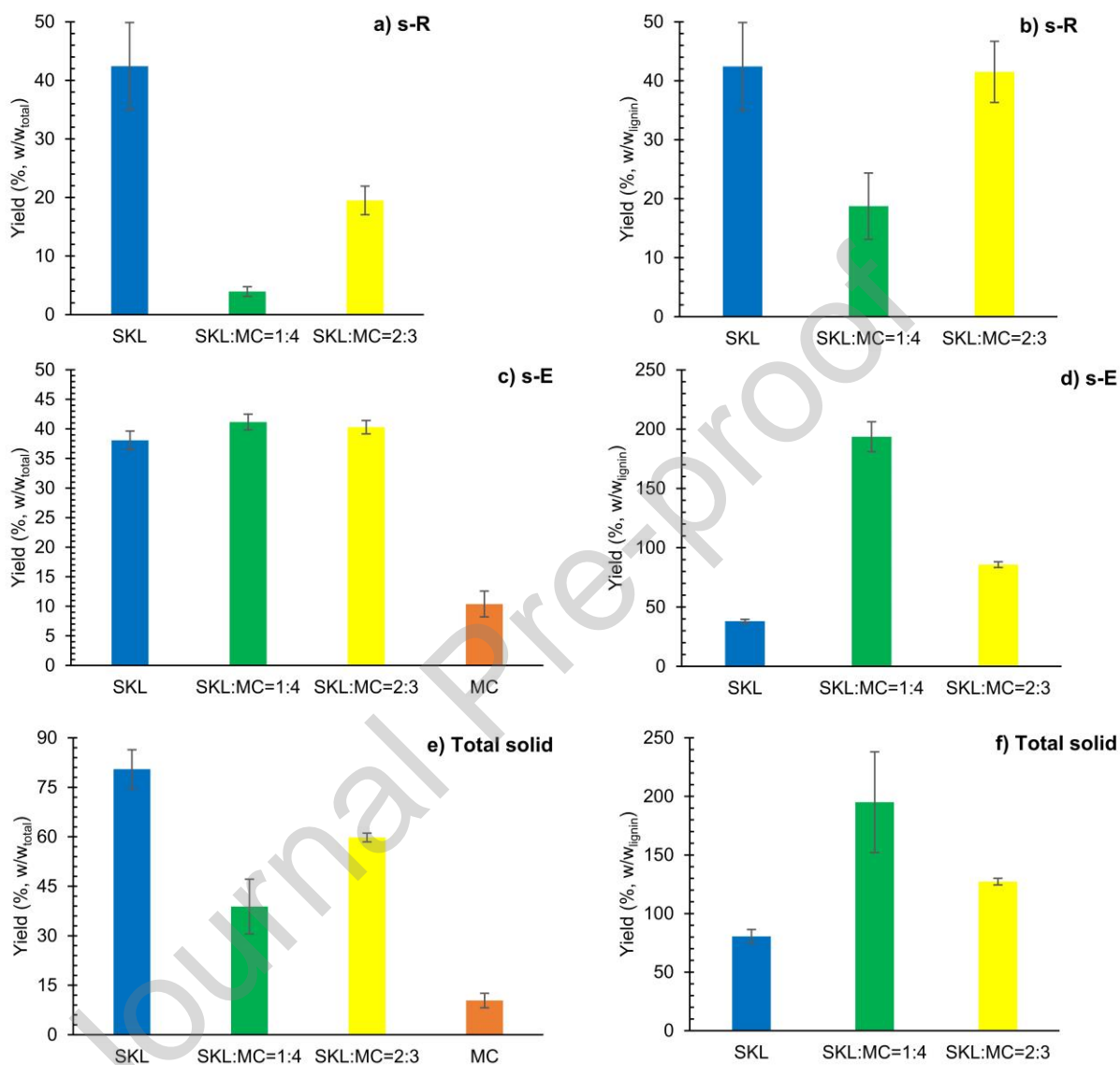

Figure 4. The yield of heavier fraction: s-R a) based on total mass b) based on lignin mass; s-E c) based on total mass d) based on lignin mass; total solid yield e) based on total mass f) based on lignin mass (error bars presented as standard error)

As mentioned above, MC are undergoing the reaction in SCW when SKL was not present inside the reaction mixture, as shown by their high conversions. After performing fractionation steps of the sample obtained with MC, the whole solid fraction was dissolved in ethyl acetate and thereby no s-R fraction is obtained while the yield of the s-E fraction is

around 10 % (Figure 4c). It is difficult to confirm whether the MC react between each other or with SKL fragments, but the experiment where the SKL:MC ratio was 2:3 yielded approximately the same amount of s-R compared to the experiment with just SKL (yield based on SKL mass, see Figure 4b), denoting that MC could polymerize with lignin fragments.

GPC chromatogram of samples obtained with MC, SKL and the mixture of MC and SKL are presented in Figure 5. Spectrum from a sample of MC shows peaks at diverse retention times, confirming a certain degree of polymerization among them, as has already been observed previously for vanillin [37]. Samples obtained with the mixture of MC and SKL (1:4 and 2:3) have peaks appearing at a shorter reaction time ($t \approx 8$ min) compared to the sample obtained with SKL. These results suggest that, at least partially, MC have reacted with SKL fragments to yield higher molecular weight compounds.
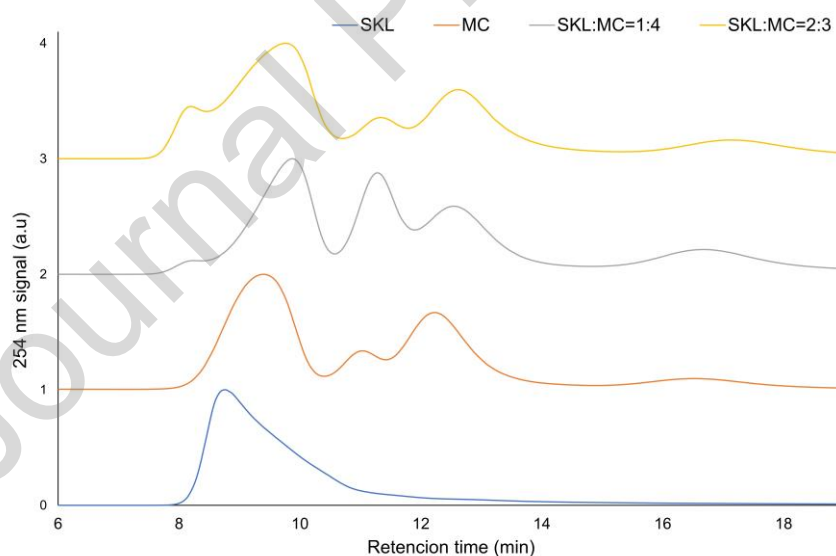
**Figure 5.** GPC chromatogram of the samples

3.3 Analysis and characterization of solid fraction

3.3.1 FT-IR analysis

FT-IR analysis of the original SKL, the s-R fraction of SKL, the s-R fraction of the mixture of MC and SKL and the s-E fraction of MC is presented in Figure 6. Every sample shows the

typical lignin signals that are assigned according to the literature[38–41]. The main change obtained in spectra of s-R fractions of SKL compared to the original SKL is the disappearance of a peak at 618 cm^{-1}, characteristic for sulphonic groups due to the de-sulphonation. The peaks between 2938 cm^{-1} and 2842 cm^{-1}, assigned to C-H stretching frequencies of aromatic methoxy group, methyl and methylene groups of the side chain have decreased intensity in s-R fraction compared to original SKL. s-E fraction of MC had the shift in the wavenumber for most of the bands. For example, aromatic skeleton vibration that appears for every s-R fraction at 1600 cm-1 and 1511 cm^{-1} is shifted to 1570 cm^{-1} and 1501 cm^{-1}, respectively. Guaiacol ring vibration and C=O stretching was shifted from 1265 cm^{-1} to 1279 cm^{-1}.
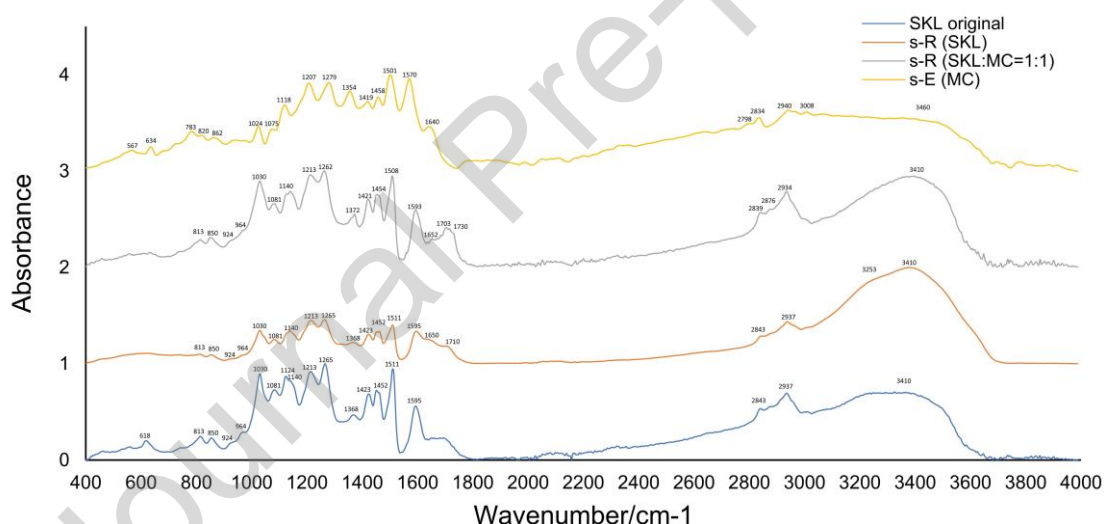
Figure 6. FT-IR spectrum of original SKL, s-R (SKL), s-R (SKL:MC=1:1) and s-E (MC)

3.3.2 HSQC analysis

The solid residue fraction (s-R) is the heaviest fraction that should contain possible re-polymerization products and unreacted lignin. Taking a detailed structural study on the s-R fraction should help us to understand the side reaction happening on SKL during the SCW process. The signals in the spectra were assigned according to previous publications [8,9,42–44].
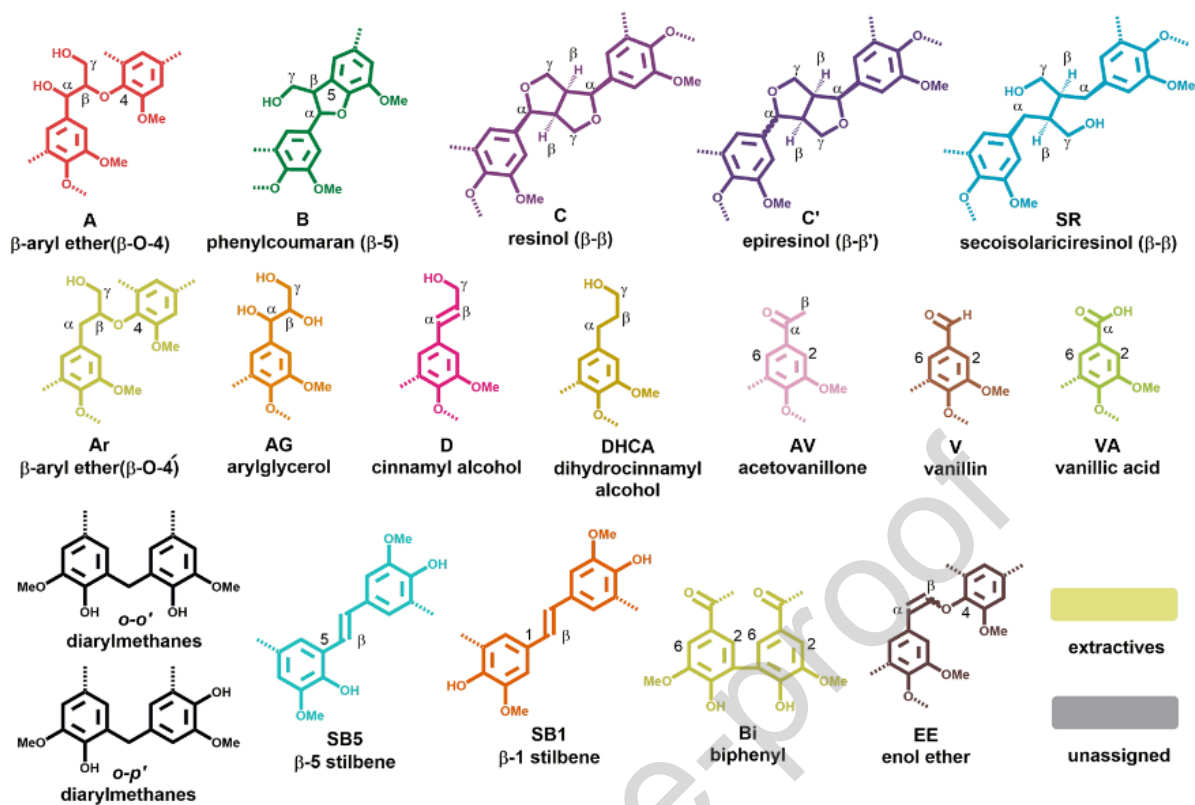
As shown in

Figure 7a HSQC spectrum of the original SKL was overlaid with its s-R fraction obtained after the SCW process. The main reaction of SKL in the SCW system was lignin de-sulphonation as the spectrum of s-R was very similar to a typical spectrum of a softwood Kraft lignin i.e., Indulin (
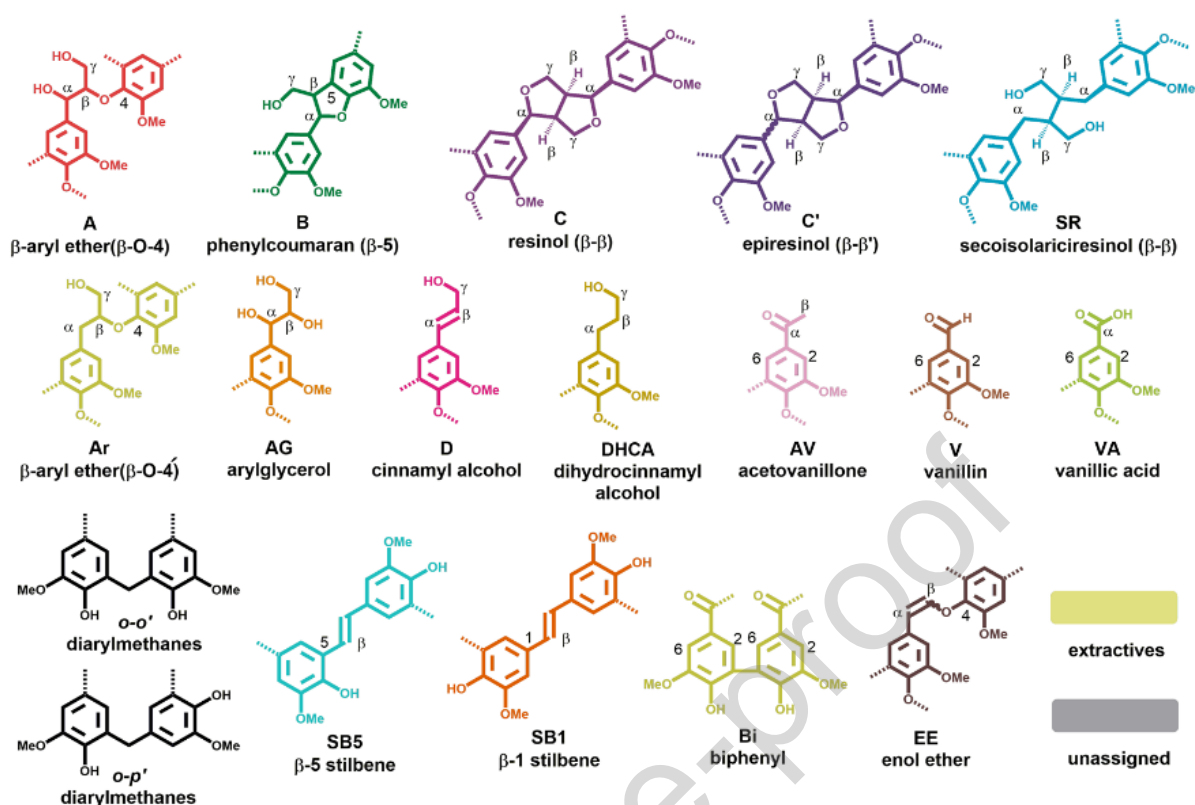
Figure 7c, f vs 6d, g). The other structural changes in SKL were rather minor and could not be investigated as they were strongly obscured by the intensive changes due to lignin de-sulphonation.
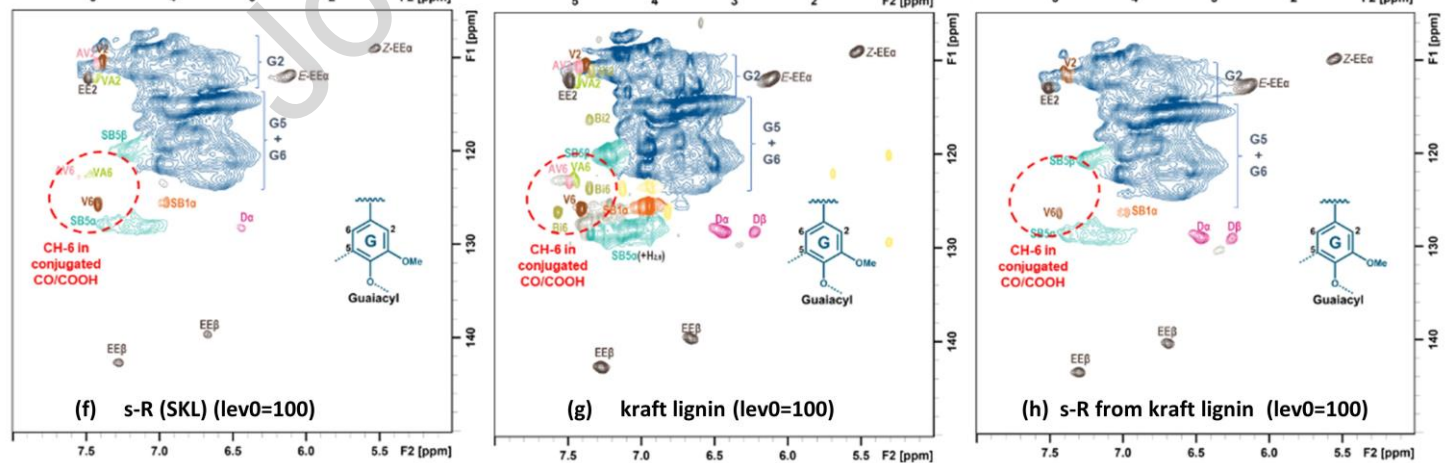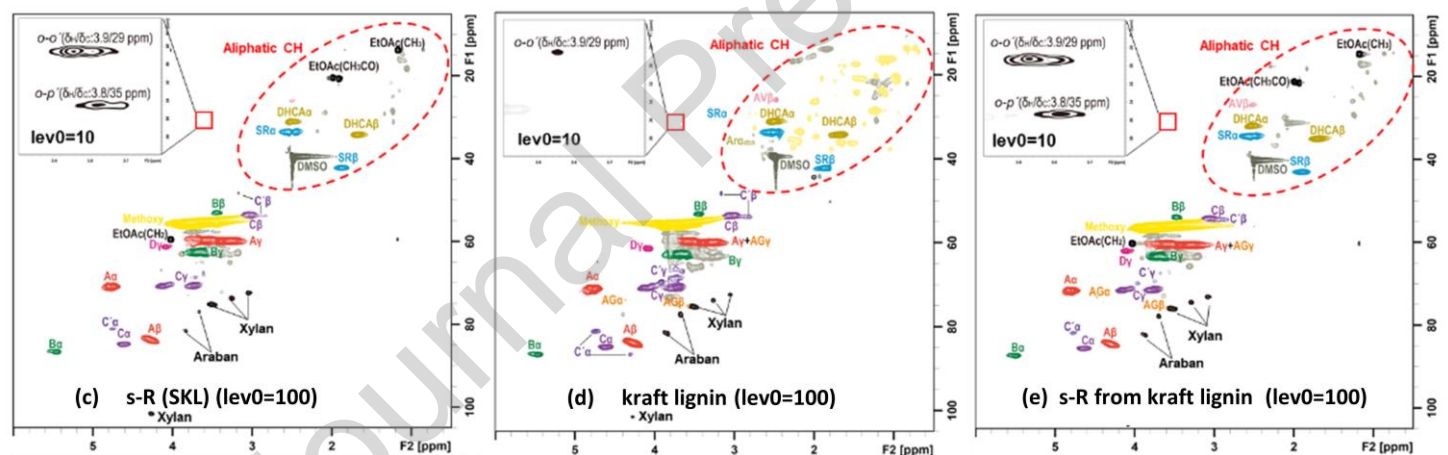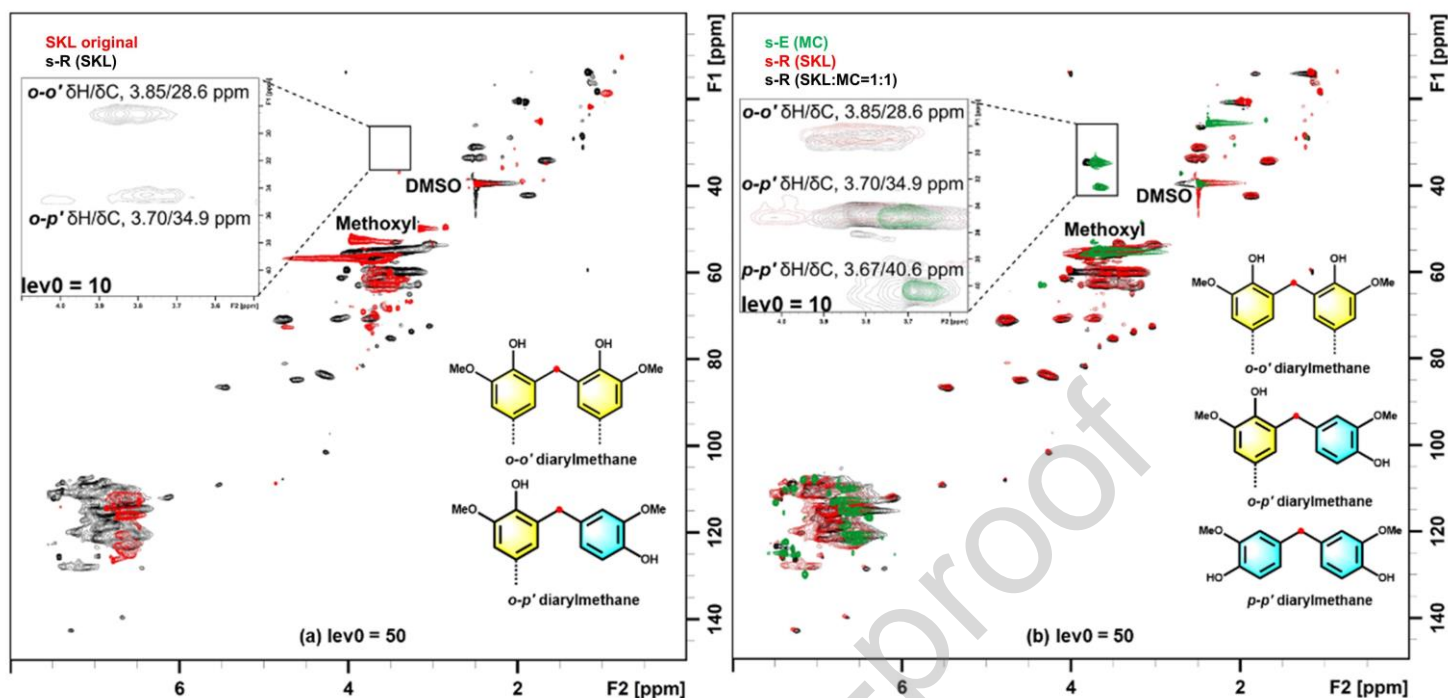
To investigate the transformation of SKL and its monomer products during the SCW process, the s-R fraction from SKL and s-E fraction of MC were compared to each other in HSQC spectra (Figure 7b). The formation of o-o′ and o-p′ diarylmethane structures with a minor amount can be observed in the s-R fraction of SKL (Figure 7a) [9,45]. In contrast, the o-p′ and p-p′ diarylmethane structures were found in the s-E fraction of MC after the SCW process (Figure 7b). This indicated that the re-polymerization can be related to the formation of diarylmethane structures, but the formation mechanism for MC and SKL is different during the SCW process. A proposal of mechanisms for the formation of diarylmethane structures from MC and SKL is presented in Figure 8a and b respectively. As shown in Figure 8a, vanillyl alcohol plays an important role in the formation of o-p′ and p-p′ diarylmethane structures. In detail, vanillyl alcohol transforms into para-quinone methide under alkaline conditions [31]. This para-quinone methide reacts at any ortho or para position to the guaiacol

generated from other monomers, finally resulting in the o-p´ and p-p´ diarylmethane, respectively. Whereas, the formation of o-o´ and o-p´ diarylmethane structures during SCW treatment on SKL may be due to the liberated formaldehyde from some structures of SKL during the SCW process, e.g., γ-position of free phenolic β-O-4 structures in the alkaline condition. Gierer and Pettersson ever reported that formaldehyde liberated from terminal hydroxymethyl groups in β-O-4 bonded quinone methide intermediates during alkaline treatment reacts with the added phenols affording the corresponding diarylmethane [46].

Therefore, we can see that the formation of p-p´ diarylmethane is limited to monomer products but hardly occur to any significant extent with polymeric lignins. On the contrary, the o-o´ diarylmethane structure was not formed among monomers. However, the formation of o-p´ and p-p´ diarylmethane structures could occur between two monomer products or/and a lignin fragment. These reactions are unlikely to directly contribute to the generation of s-R fraction from SKL during the SCW process but are beneficial to the oil fractions. Product fractionation also shows that MC contribute to the yield of total solid mainly through increased yield of s-E fraction. However, it cannot be excluded that the resultant dimeric p-p´ diarylmethane structures or low molecular lignin fragments with o-p´ diarylmethane structures would react furtherly to contribute to the s-R fractions. We assumed that the produced monomer products from SKL could involve the formation of the s-R fraction during SCW. To confirm this, the experiment with the mixture of SKL and MC was processed with SCW (SKL:MC = 1:1, Figure 7b). Interestingly, all three types of diarylmethane structures were observed in their s-R fraction, indicating all of them are related to the production of the s-R fraction during SCW. Nevertheless, p-p´ diarylmethane structures were still not found in the s-R fraction of SKL after the SCW process. It is possible that the transformation to vanillic acid for vanillyl alcohol is easier than the para quinone methide during the SCW process on SKL, thus leaving few opportunities to form the p-p´ diarylmethane structures.

Detailed kinetic studies with MC are therefore needed to address this hypothesis. The colored

structures in Figure 7 are used to show the main structural linkages in lignin samples.

(a) lev0 = 50

(b) lev0 = 50

(c) s-R (SKL) (lev0=100)

(d) kraft lignin (lev0=100)

(e) s-R from kraft lignin (lev0=100)

(f) s-R (SKL) (lev0=100)

(g) kraft lignin (lev0=100)
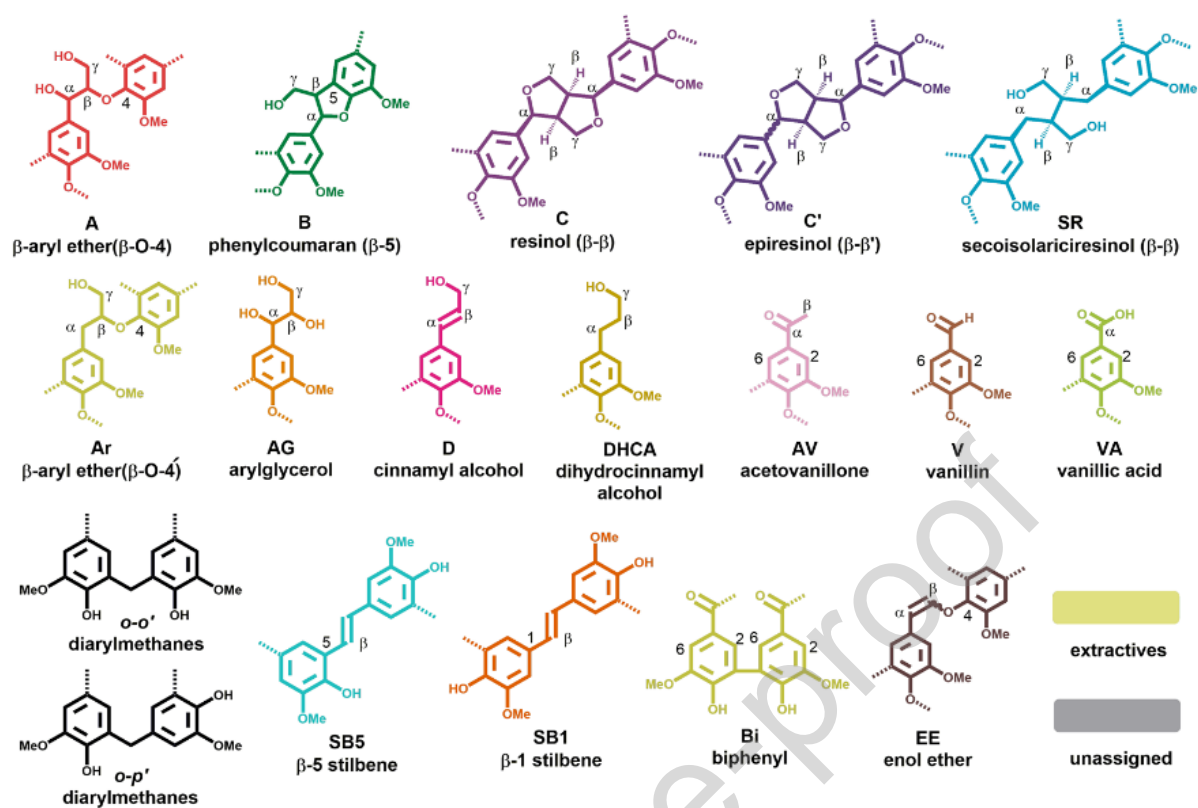
(h) s-R from kraft lignin (lev0=100)

Figure 7. 2D HSQC NMR spectra of lignin samples: SKL overlaid with its s-R fraction after SCW process (a); the s-E fraction of model compounds, the s-R fraction of SKL and their mixture after SCW process overlaid with each other (b); aliphatic region of s-R from SKL (c), Kraft lignin (d) and its s-R fraction (e); aromatic region of s-R from SKL (f), Kraft lignin (g) and its s-R fraction (h), the lev0 is the value of lowest contour level in the spectrum, the colored structures are used to show main structural linkages in lignin samples
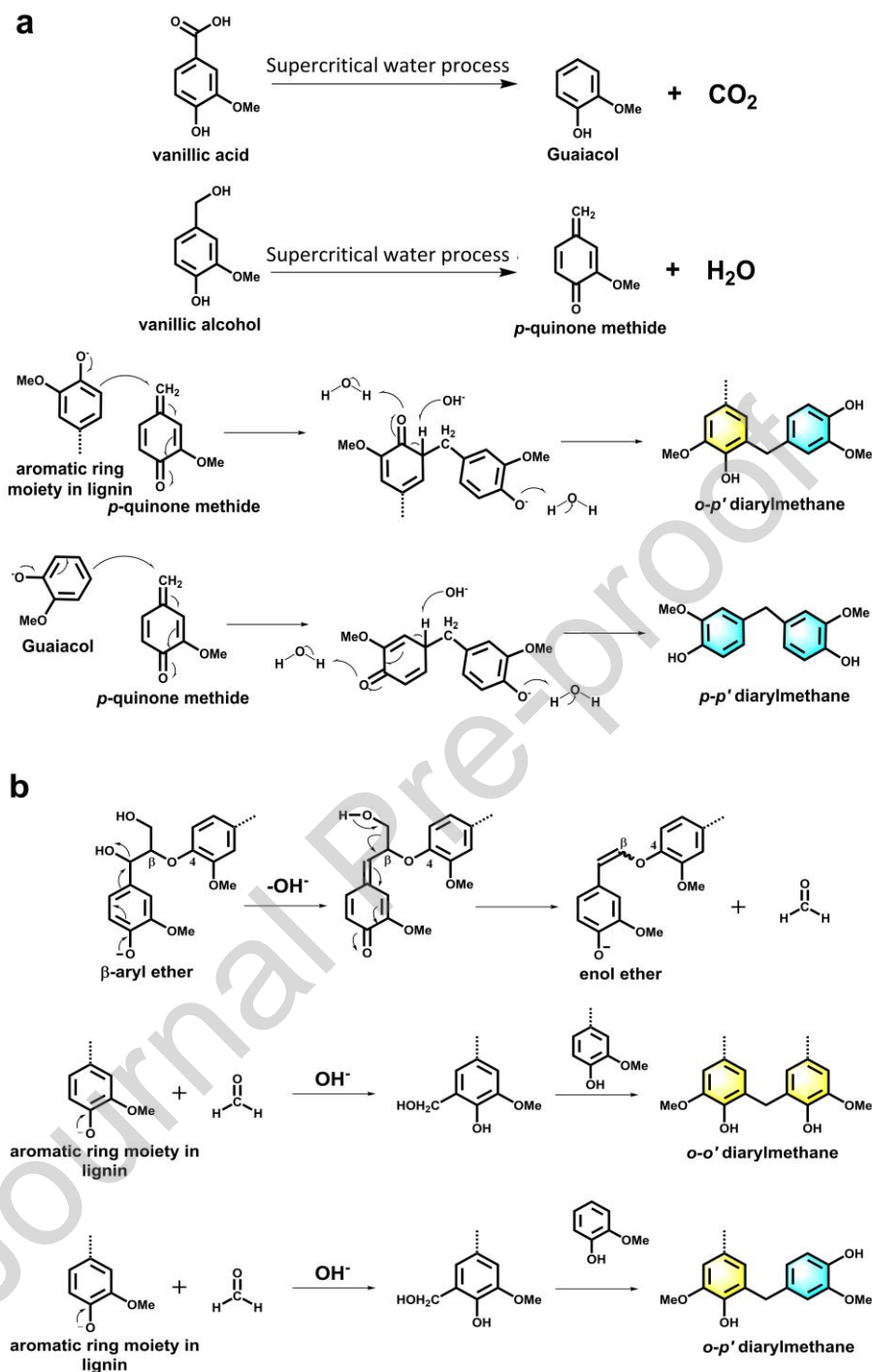
Figure 8. Proposed mechanisms for the formation of diarylmethane structures in SCW process: from MC (a); from SKL (b)

As it was very difficult to elucidate lignin re-polymerization using SKL, we performed an experiment on Kraft lignin with a much simpler structure. The structural assignment of HSQC spectra of original Kraft lignin (Indulin), and its s-R fraction after the SCW process are

presented in Figure 7 (d/g, e/h). Their main structural quantitative data are shown in Table 2. In the s-R fractions obtained from Kraft lignin after the SCW process, a small amount of o-o′ diarylmethane structures as crosslinked bridges between two lignin fragments can be observed. Therefore, these diarylmethane structures may contribute to the formation of s-R fractions from Kraft lignins after the SCW process. Although our data in Table 2 shows a small amount of o-o′ diarylmethane structure (0.5%) in the s-R from Kraft lignin, they are sufficient to cross-link the lignin fragments to double the molecular weight of resultant solid residue. Also, no new Alk-Ar structures were observed in the spectrum of Kraft lignin after the reaction. However, the formation of Ar-Ar and/or Ar-O-Ar (e.g., 5-5', 4-O-5') moieties contributing to the production of s-R fraction during the SCW process cannot be excluded as the HSQC technique does not allow their reliable analysis.

There is no significant difference observed in the oxygenated alkyl region between Kraft lignin and its s-R fractions after the SCW process (Figure 7d, e). This indicates that cross-polymerization may happen between lignin fragments after the SCW process. Consequently, their main inter-structural linkages were preserved. Figure 7 shows a remarkable similarity between the original Kraft lignin and its s-R fraction after the reaction. Most of the differences were within the experimental error or/and related to very minor lignin moieties. The only noticeable difference was a decrease in the amount of stilbene moieties (from ca 25/100 Ar to about 10/100Ar), which apparently underwent degradation in the SWC process.

Table 2. Amount of typical inter-unit linkages in samples (nlev = 50, lev0 = 20, toplev = 100 %)

No.	HSQC peaks	Indulin/100 aromatic ring	s-R from Indulin/100 aromatic ring	Assignment
1	Methoxyl	105.5	110.6	-OCH3
2	G2	100.0	100	CH-2 in Guaiacyl ring
3	Aα	9.8	7.9	β-O-4

4	Bα	3.0	3.2	β-5
5	Cα	2.1	1.8	β-β
6	C'α	0.9	0.9	epiresinol
7	SRβ	2.5	2.5	secoisolariciresinol
8	Arα	0.7	0.8	Reduced β-O-4
9	AGα	0.5	1.2	arylglycerol
10	Dγ	1.7	1.6	cinnamyl alcohol
11	DHCAβ	3.9	4.3	dihydrocinnamyl
12	AVβ	0.5	0.8	acetovanillone
13	*o-o′*	0.1	0.3	diarylmethane
14	*o-p′*	ND	0.1	diarylmethane
15	V6	1.8	0.9	vanillin
16	VA6	0.8	ND	Vanillic acid
17	E-EEα	2.4	3.0	E-Enol ether
18	Z-EEα	1.2	1.1	Z-Enol ether
19	SB1α	2.5	0.7	β-1 stilbene
20	SB5β	19.8	8.2	β-5 stilbene

4. Conclusion

Lignin model compounds tend to furtherly react in SCW as shown by their high conversions, both between themselves and with lignin fragments. The yield of the solid fraction increases when the mixture of SKL and MC is processed in SCW, compared to the processing of just SKL, signifying that MC contribute to solid formation. To reduce the re-polymerization and recover the high yield of monomers in the SCW process, light oil fraction enriched in monomers should be separated from the reaction mixture as soon as it is produced.

One of the products found in the solid extract fraction of MC and solid residue fraction obtained with SKL are diarylmethanes structures. The formation of those moieties contributes

to the re-polymerization but their mechanism pathway is different for SKL and MC. After SCW processing SKL residue has a structure similar to softwood Kraft lignin and the main reaction that occurred is SKL de-sulphonation. Noteworthy, the chemical structure of Indulin Kraft lignin and its solid residue after the SCW process were remarkably similar indicating that the main reactions occurred in the fractions of low molecular weight products.

Declaration of interests

☒ The authors declare that they have no known competing financial interests or personal relationships that could have appeared to influence the work reported in this paper.

☐ The authors declare the following financial interests/personal relationships which may be considered as potential competing interests:

References:

(1)   Ma, J.; Jin, D.; Li, Y.; Xiao, D.; Jiao, G.; Liu, Q.; Guo, Y.; Xiao, L.; Chen, X.; Li, X.; Zhou, J.; Sun, R. Photocatalytic Conversion of Biomass-Based Monosaccharides to Lactic Acid by Ultrathin Porous Oxygen Doped Carbon Nitride. *Appl. Catal. B Environ.* **2021**, *283*, 119520. https://doi.org/10.1016/j.apcatb.2020.119520.

(2)   de Jong, E.; Higson, A.; Walsh, P.; Wellisch, M. Bio-Based Chemicals Value Added Products from Biorefineries. *IEA Bioenergy – Task 42 Biorefinery* **2011**.

(3)   Holladay, J. E.; White, J. F.; Bozell, J. J.; Johnson, D. Top Value-Added Chemicals

from Biomass Volume II—Results of Screening for Potential Candidates from Biorefinery Lignin. *Off. Sci. Tech. Inf.* **2007**, *II* (October), 69.

(4) Wenger, J.; Haas, V.; Stern, T. Why Can We Make Anything from Lignin Except Money? Towards a Broader Economic Perspective in Lignin Research. *Curr. For. Reports* **2020**, *6* (4), 294–308. https://doi.org/10.1007/s40725-020-00126-3.

(5) Rinaldi, R.; Jastrzebski, R.; Clough, M. T.; Ralph, J.; Kennema, M.; Bruijnincx, P. C. A.; Weckhuysen, B. M. Paving the Way for Lignin Valorisation: Recent Advances in Bioengineering, Biorefining and Catalysis. *Angew. Chemie - Int. Ed.* **2016**, *55* (29), 8164–8215. https://doi.org/10.1002/anie.201510351.

(6) Mboowa, D. A Review of the Traditional Pulping Methods and the Recent Improvements in the Pulping Processes. *Biomass Convers. Biorefinery* **2021**. https://doi.org/10.1007/s13399-020-01243-6.

(7) Azadi, P.; Inderwildi, O. R.; Farnood, R.; King, D. A. Liquid Fuels, Hydrogen and Chemicals from Lignin: A Critical Review. *Renew. Sustain. Energy Rev.* **2013**, *21*, 506–523. https://doi.org/10.1016/j.rser.2012.12.022.

(8) Kyosti V Sarkanen, C. H. L. *Wood Chemistry: Lignins. Occurrence, Formation, Structure, and Reactions*; 1971. https://doi.org/10.1126/science.175.4025.978-b.

(9) Lancefield, C. S.; Wienk, H. L. J.; Boelens, R.; Weckhuysen, B. M.; Bruijnincx, P. C. A. Identification of a Diagnostic Structural Motif Reveals a New Reaction Intermediate and Condensation Pathway in Kraft Lignin Formation. *Chem. Sci.* **2018**, *9* (30), 6348–6360. https://doi.org/10.1039/C8SC02000K.

(10) Balakshin, M. Y.; Capanema, E. A.; Chen; Gracz, H. S. Elucidation of the Structures of Residual and Dissolved Pine Kraft Lignins Using an HMQC NMR Technique. *J. Agric.*

Food Chem. **2003**, *51* (21), 6116–6127. https://doi.org/10.1021/jf034372d.

(11) Chakar, F. S.; Ragauskas, A. J. Review of Current and Future Softwood Kraft Lignin Process Chemistry. *Ind. Crops Prod.* **2004**, *20* (2), 131–141. https://doi.org/10.1016/j.indcrop.2004.04.016.

(12) Aro, T.; Fatehi, P. Production and Application of Lignosulfonates and Sulfonated Lignin. *ChemSusChem* **2017**, *10* (9), 1861–1877. https://doi.org/10.1002/cssc.201700082.

(13) Chio, C.; Sain, M.; Qin, W. Lignin Utilization: A Review of Lignin Depolymerization from Various Aspects. *Renew. Sustain. Energy Rev.* **2019**, *107* (December 2018), 232–249. https://doi.org/10.1016/j.rser.2019.03.008.

(14) Xu, C.; Arancon, R. A. D.; Labidi, J.; Luque, R. Lignin Depolymerisation Strategies: Towards Valuable Chemicals and Fuels. *Chem. Soc. Rev.* **2014**, *43* (22), 7485–7500. https://doi.org/10.1039/c4cs00235k.

(15) Roy, R.; Rahman, S.; Amit, T. A. Recent Advances in Lignin Depolymerization Techniques : A Comparative Overview of Traditional and Greener Approaches. **2022**, 130–154.

(16) Cocero, M. J.; Cabeza, Á.; Abad, N.; Adamovic, T.; Vaquerizo, L.; Martínez, C. M.; Pazo-Cepeda, M. V. Understanding Biomass Fractionation in Subcritical & Supercritical Water. *J. Supercrit. Fluids* **2018**, *133*, 550–565. https://doi.org/10.1016/j.supflu.2017.08.012.

(17) Jiang, W.; Lyu, G.; Wu, S.; Lucia, L. A.; Yang, G.; Liu, Y. Supercritical Water-Induced Lignin Decomposition Reactions: A Structural and Quantitative Study. *BioResources* **2016**, *11* (3). https://doi.org/10.15376/biores.11.3.5660-5675.

(18) Saisu, M.; Sato, T.; Watanabe, M.; Adschiri, T.; Arai, K. Conversion of Lignin with Supercritical Water−Phenol Mixtures. *Energy & Fuels* **2003**, *17* (4), 922–928. https://doi.org/10.1021/ef0202844.

(19) Wahyudiono; Sasaki, M.; Goto, M. Recovery of Phenolic Compounds through the Decomposition of Lignin in near and Supercritical Water. *Chem. Eng. Process. Process Intensif.* **2008**, *47* (9–10), 1609–1619. https://doi.org/10.1016/j.cep.2007.09.001.

(20) Yong, T. L.-K.; Matsumura, Y. Reaction Kinetics of the Lignin Conversion in Supercritical Water. *Ind. Eng. Chem. Res.* **2012**, *51* (37), 11975–11988. https://doi.org/10.1021/ie300921d.

(21) Pérez, E.; Tuck, C. O. Quantitative Analysis of Products from Lignin Depolymerisation in High-Temperature Water. *Eur. Polym. J.* **2018**, *99*, 38–48. https://doi.org/10.1016/j.eurpolymj.2017.11.053.

(22) Ahlbom, A.; Maschietti, M.; Nielsen, R.; Hasani, M.; Theliander, H. Towards Understanding Kraft Lignin Depolymerisation under Hydrothermal Conditions. *Holzforschung* **2021**. https://doi.org/10.1515/hf-2021-0121.

(23) Cantero, D. A.; Bermejo, M. D.; Cocero, M. J. Governing Chemistry of Cellulose Hydrolysis in Supercritical Water. *ChemSusChem* **2015**, *8* (6), 1026–1033. https://doi.org/10.1002/cssc.201403385.

(24) Brunner, G. *Hydrothermal and Supercritical Water Processes*; Elsevier, 2014.

(25) Okuda, K.; Ohara, S.; Umetsu, M.; Takami, S.; Adschiri, T. Disassembly of Lignin and Chemical Recovery in Supercritical Water and P-Cresol Mixture. Studies on Lignin Model Compounds. *Bioresour. Technol.* **2008**, *99* (6), 1846–1852. https://doi.org/10.1016/j.biortech.2007.03.062.

(26)   Okuda, K.; Man, X.; Umetsu, M.; Takami, S.; Adschiri, T. Efficient Conversion of Lignin into Single Chemical Species by Solvothermal Reaction in Water-p-Cresol Solvent. *J. Phys. Condens. Matter* **2004**, *16* (14). https://doi.org/10.1088/0953-8984/16/14/045.

(27)   Saisu, M.; Sato, T.; Watanabe, M.; Adschiri, T.; Arai, K. Conversion of Lignin with Supercritical Water-Phenol Mixtures. *Energy and Fuels* **2003**, *17* (4), 922–928. https://doi.org/10.1021/ef0202844.

(28)   Okuda, K.; Umetsu, M.; Takami, S.; Adschiri, T. Disassembly of Lignin and Chemical Recovery—Rapid Depolymerization of Lignin without Char Formation in Water–Phenol Mixtures. *Fuel Process. Technol.* **2004**, *85* (8–10), 803–813. https://doi.org/10.1016/j.fuproc.2003.11.027.

(29)   Abad-Fernández, N.; Pérez, E.; Cocero, M. J. Aromatics from Lignin through Ultrafast Reactions in Water. *Green Chem.* **2019**, *21* (6), 1351–1360. https://doi.org/10.1039/c8gc03989e.

(30)   Cantero, D. A.; Bermejo, M. D.; Cocero, M. J. Kinetic Analysis of Cellulose Depolymerization Reactions in near Critical Water. *J. Supercrit. Fluids* **2013**, *75*, 48–57. https://doi.org/10.1016/j.supflu.2012.12.013.

(31)   Komatsu, T.; Yokoyama, T. Revisiting the Condensation Reaction of Lignin in Alkaline Pulping with Quantitativity Part I: The Simplest Condensation between Vanillyl Alcohol and Creosol under Soda Cooking Conditions. *J. Wood Sci.* **2021**, *67* (1), 45. https://doi.org/10.1186/s10086-021-01978-4.

(32)   Pérez, E.; Tuck, C. O. Quantitative Analysis of Products from Lignin Depolymerisation in High-Temperature Water. *Eur. Polym. J.* **2018**, *99* (December 2017), 38–48. https://doi.org/10.1016/j.eurpolymj.2017.11.053.

(33)   Pérez, E.; Abad-Fernández, N.; Lourençon, T.; Balakshin, M.; Sixta, H.; Cocero, M. J. Base-Catalysed Depolymerization of Lignins in Supercritical Water: Influence of Lignin Nature and Valorisation of Pulping and Biorefinery by-Products. *Biomass and Bioenergy* **2022**, *163*, 106536. https://doi.org/10.1016/j.biombioe.2022.106536.

(34)   González, G.; Salvadó, J.; Montané, D. Reactions of Vanillic Acid in Sub- and Supercritical Water. *J. Supercrit. Fluids* **2004**, *31* (1), 57–66. https://doi.org/10.1016/j.supflu.2003.09.015.

(35)   Abad-Fernández, N.; Pérez, E.; Martín, Á.; Cocero, M. J. Kraft Lignin Depolymerisation in Sub- and Supercritical Water Using Ultrafast Continuous Reactors. Optimization and Reaction Kinetics. *J. Supercrit. Fluids* **2020**, *165*. https://doi.org/10.1016/j.supflu.2020.104940.

(36)   Liu, C.; Deng, Y.; Wu, S.; Mou, H.; Liang, J.; Lei, M. Study on the Pyrolysis Mechanism of Three Guaiacyl-Type Lignin Monomeric Model Compounds. *J. Anal. Appl. Pyrolysis* **2016**, *118*, 123–129. https://doi.org/10.1016/j.jaap.2016.01.007.

(37)   Pérez, E.; Tuck, C. O. Quantitative Analysis of Products from Lignin Depolymerisation in High-Temperature Water. *Eur. Polym. J.* **2018**, *99*, 38–48. https://doi.org/10.1016/j.eurpolymj.2017.11.053.

(38)   Hemmilä, V.; Hosseinpourpia, R.; Adamopoulos, S.; Eceiza, A. Characterization of Wood-Based Industrial Biorefinery Lignosulfonates and Supercritical Water Hydrolysis Lignin. *Waste and Biomass Valorization* **2020**, *11* (11), 5835–5845. https://doi.org/10.1007/s12649-019-00878-5.

(39)   Pang, B.; Yang, S.; Fang, W.; Yuan, T. Q.; Argyropoulos, D. S.; Sun, R. C. Structure-Property Relationships for Technical Lignins for the Production of Lignin-Phenol-Formaldehyde Resins. *Ind. Crops Prod.* **2017**, *108* (March), 316–326.

https://doi.org/10.1016/j.indcrop.2017.07.009.

(40) Constant, S.; Wienk, H. L. J.; Frissen, A. E.; Peinder, P. De; Boelens, R.; Van Es, D. S.; Grisel, R. J. H.; Weckhuysen, B. M.; Huijgen, W. J. J.; Gosselink, R. J. A.; Bruijnincx, P. C. A. New Insights into the Structure and Composition of Technical Lignins: A Comparative Characterisation Study. *Green Chem.* **2016**, *18* (9), 2651–2665. https://doi.org/10.1039/c5gc03043a.

(41) Boeriu, C. G.; Fiţigău, F. I.; Gosselink, R. J. A.; Frissen, A. E.; Stoutjesdijk, J.; Peter, F. Fractionation of Five Technical Lignins by Selective Extraction in Green Solvents and Characterisation of Isolated Fractions. *Ind. Crops Prod.* **2014**, *62*, 481–490. https://doi.org/10.1016/j.indcrop.2014.09.019.

(42) *Lignin and Lignans*; Heitner, C., Dimmel, D. R., Schmidt, J. A., Eds.; CRC Press, 2016.

(43) Boeriu, C. G.; Fiţigău, F. I.; Gosselink, R. J. A.; Frissen, A. E.; Stoutjesdijk, J.; Peter, F. Fractionation of Five Technical Lignins by Selective Extraction in Green Solvents and Characterisation of Isolated Fractions. *Ind. Crops Prod.* **2014**, *62*, 481–490. https://doi.org/10.1016/j.indcrop.2014.09.019.

(44) Capanema, E. A.; Balakshin, M. Y.; Chen, C.-L.; Gratzl, J. S.; Gracz, H. Structural Analysis of Residual and Technical Lignins by 1H-13C Correlation 2D NMR-Spectroscopy. *Holzforschung* **2001**, *55* (3), 302–308. https://doi.org/10.1515/HF.2001.050.

(45) Yelle, D. J.; Ralph, J. Characterizing Phenol–Formaldehyde Adhesive Cure Chemistry within the Wood Cell Wall. *Int. J. Adhes. Adhes.* **2016**, *70*, 26–36. https://doi.org/10.1016/j.ijadhadh.2016.05.002.

(46)   Gierer, J.; Pettersson, I. Studies on the Condensation of Lignins in Alkaline Media. Part

II. The Formation of Stilbene and Arylcoumaran Structures through Neighbouring

Group Participation Reactions. *Can. J. Chem.* **1977**, *55* (4), 593–599.

https://doi.org/10.1139/v77-084.

Graphical abstract
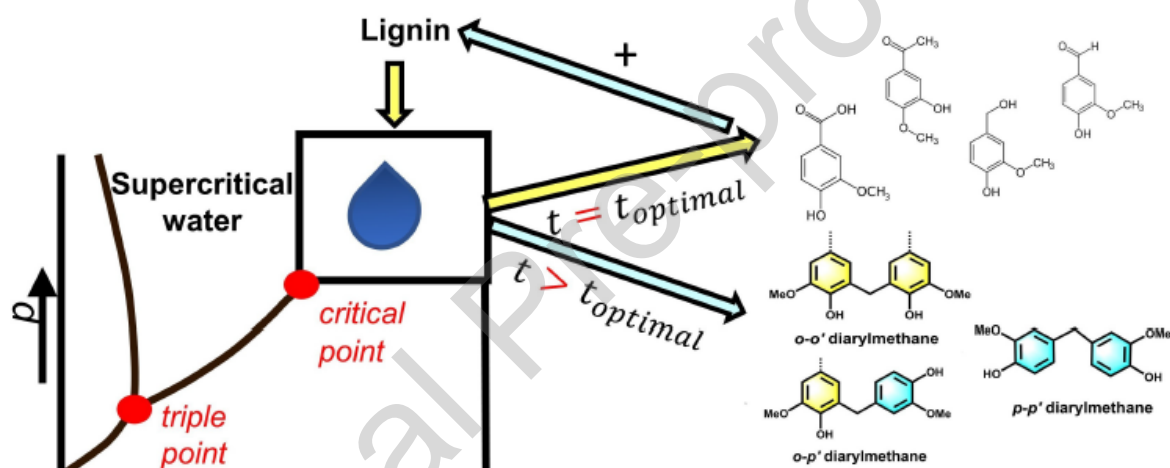
Highlights
- Study on the role of model compounds to lignin re-polymerization in supercritical water
- Reactivity of model compounds with and without sulfonated kraft lignin was followed
- The presence of model compounds cause an increased yield of heavier fractions
- The formation of diarylmethane structures was assigned to lignin re-polymerization
- Reaction mechanism for diarylmethanes formation is proposed